NANO LETTERS

2007
Vol. 7, No. 11
3512−3517

Synthesis, Characterization, and Optical Properties of Ordered Arrays of III-Nitride Nanocrystals

Sreekar Bhaviripudi,[†] Jifa Qi,[†] Evelyn L. Hu,[§] and Angela M. Belcher*[,†,‡]

Department of Materials Science and Engineering, Department of Biological Engineering, Massachusetts Institute of Technology, Cambridge, Massachusetts 02139, and Department of Electrical and Computer Engineering, Department of Materials, University of California, Santa Barbara, California 93106

Received August 23, 2007; Revised Manuscript Received October 5, 2007

ABSTRACT

A new approach involving self-assembling block copolymer micellar templates and gas-phase reactions to synthesize arrays of monodisperse III-nitrides nanocrystals in the size range of 1–5 nm with uniform spacings between the nanoparticles is demonstrated. The photoluminescence emission spectra revealed the GaN nanocrystals are in the quantum-confined regime. This method not only offers great promise for the controlled synthesis of arrays of ternary III-nitride nanocrystals but may also enable doping in binary nitrides.

III-Nitrides have received immense attention over the past decade as potential materials with successful opto-electronic applications.[1−3] For example, GaN nanostructures including nanocrystals and nanowires with size less than 10 nm (Bohr-exciton radius 2−10 nm)[4−5] exhibit interesting optical properties largely due to quantum confinement effects. Current efforts are focused on the synthesis as well as on understanding the physical properties of crystalline GaN nanoparticles. Investigations on the synthesis of GaN nanoparticles including colloidal methods,[4] solvo-thermal methods,[6−7] detonation of gallium azide and cyclotrigallazanes,[8−11] metallo-organic chemical vapor deposition (MOCVD)[12] and molecular beam epitaxial methods,[13] have been previously reported. However, despite significant progress in the synthesis of GaN nanoparticles using different methods it is still a challenge to synthesize nanoparticles with controlled size and shape uniformity in the 1−5 nm range. Moreover, in many cases the nanoparticles tend to agglomerate, making it difficult to study the optical properties from individual isolated nanoparticles. Though MOCVD and molecular beam epitaxy (MBE) methods offer good control over the size of the nanoparticles, these methods are limited by the need for lattice-matched substrates and are relatively more expensive. Here, a new approach involving block copolymer (BCP) templates in conjunction with gas-phase reactions has been employed to synthesize uniform arrays of monodisperse III-nitride nanocrystals, including GaN and InN. The unique advantage of this approach involves simultaneous control over the size and the spacings between the III-nitride nanocrystals that is offered by the BCP templates. In addition, the gas-phase reactions could be tailored by controlling the reaction parameters (pressure, temperature, and composition of ambient gas) to either modify the surface of nanocrystals or enable doping in nitride nanostructures. This method not only offers promise for the controlled synthesis of ternary III-N nanocrystals but may also enable doping in III-nitrides nanostructures.

In this work, syntheses of ordered arrays of III-nitride nanocrystals including GaN and InN with average sizes in the range of 1−5 nm on different substrates using polystyrene-b-poly(4-vinylpyridine) (PS-P4VP) diblock copolymer micellar templates is reported. A block copolymer consists of a chain of two distinct immiscible monomers that phase separate to form nanometer-sized domains. They can be self-assembled to form structures with various geometries, which have been widely used as templates to synthesize inorganic nanoscale materials.[14−15] Diblock copolymer micelles have been used as nanoreactors to synthesize ordered arrays of noble metal nanoparticles on different substrates,[16−18] and recently synthesis of mono- and bimetallic nanoparticles using the same approach have also been reported.[19] While many investigations so far have focused on the synthesis of transition metal nanoparticles using this method, in this work the versatility of the BCP method to synthesize ordered oxide and nitride nanocrystal arrays of metallic p-block elements

* To whom correspondence should be addressed. E-mail: belcher@mit.edu.
[†] Department of Materials Science and Engineering, Massachusetts Institute of Technology.
[‡] Department of Biological Engineering, Massachusetts Institute of Technology.
[§] University of California.

10.1021/nl072129d CCC: $37.00
Published on Web 10/19/2007

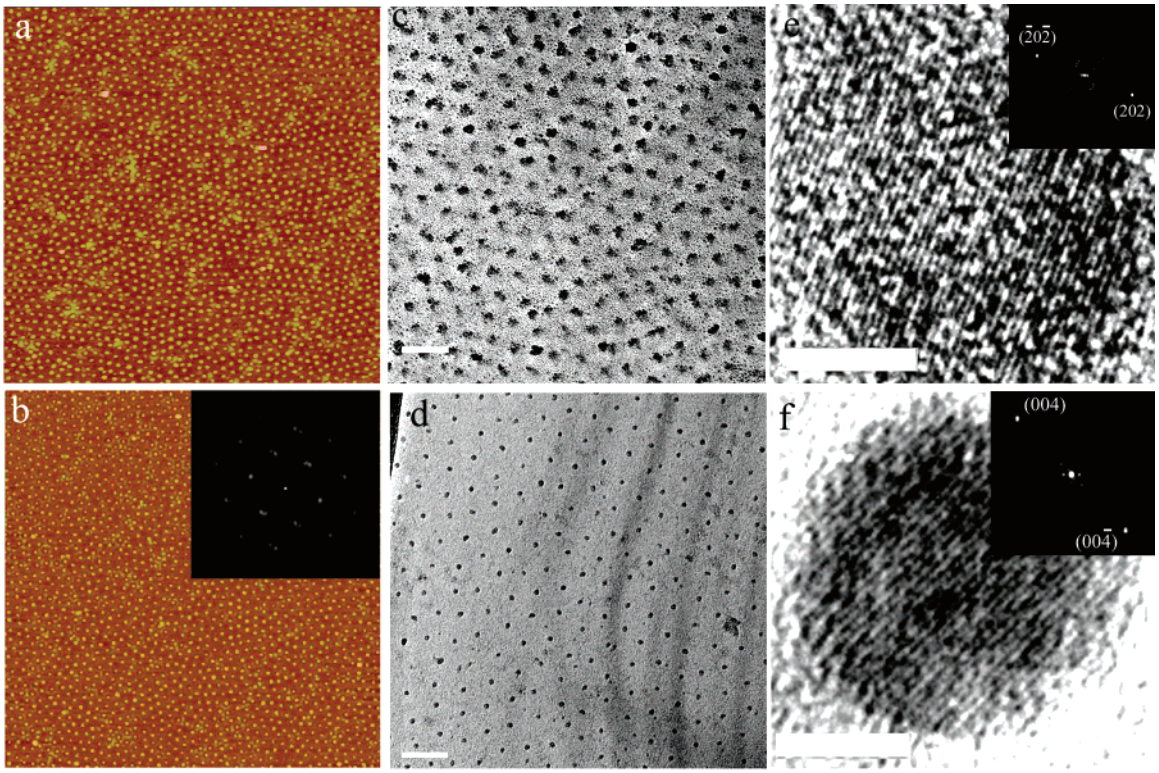

Figure 1. AFM height images (2.5 × 2.5 μm^2) of (a) Ga_2O_3 nanoparticles and (b) GaN nanoparticles on Si substrates obtained after O_2 and N_2 plasma treatments, respectively. Inset in (b) is a FFT. TEM images of GaN nanoparticles on Si substrate (c) obtained by ammonia treatment of Ga_2O_3 nanoparticles at 650 °C (scale bar 100 nm) (d) obtained by N_2 plasma treatment followed by annealing in ammonia gas at 700 °C (scale bar 100 nm). FFTs are shown as insets in the corresponding images. High-resolution TEM images of corresponding GaN nanoparticles synthesized are shown in (e) and (d), respectively, ((e,f) scale bar 2 nm).

(Ga and In) using PS-P4VP block copolymer is also demonstrated.

First, PS-P4VP micellar solution was prepared by adding 0.2 g of PS-P4VP (M_n-PS-b-P4VP, 20000-b-19000; PDI, 1.09; Polymer Source, Inc.) to 50 mL of toluene (Alfa Aesar) and was stirred at 70 °C for 4 h. Gallium nitrate [$Ga(NO_3)_3 \cdot xH_2O$, 99.999%] (Sigma Aldrich) (6 mg) and gallium(III) acetylacetonoate [$(C_5H_8O_2)_3Ga$, 99.99%] (Aldrich) (9 mg) (referred to as GaAc) precursors were each added to 25 mL of the polymer micellar solution and stirred for 12 h at room temperature. Reverse micelles of PS-P4VP di-block copolymer were formed in toluene consisting of polar P4VP cores in nonpolar PS domains that are capable of self-organizing into ordered structures on substrates. Interactions between the nonbonding electrons on the nitrogen in the pyridine block and the partially filled p-orbitals of these metallic p-block elements resulted in the formation of coordinate covalent bonds that were utilized to sequester metal precursors into the core of the micelles (see Supporting Information). These metal precursor-loaded polymer solutions were then spin-coated on three different substrates: sapphire, 100 nm of silicon dioxide thermally grown on boron-doped p-type Si (100) (henceforth referred to as Si substrates), and fused silica glass substrates. Spin-coating of metal precursor loaded polymer micelles resulted in the formation of a monolayer of micelles along a hexagonal arrangement. After spin-coating, the polymeric layer was removed using either oxygen or nitrogen plasma (300−500 mtorr, 5 min) (Harrick, Plasma Sterilizer, PDC-32G) that also resulted in the formation of arrays of Ga_2O_3 and GaN nanoparticles, respectively.

The size and the periodicity of the nanoparticles that were obtained after oxygen and nitrogen plasma treatments were determined using atomic force microscopy (AFM) studies. AFM studies were carried out using a Nanoscope IV (Digital Instruments) in the tapping mode under ambient conditions using silicon cantilever tips (radius of curvature ranging between 5 and 10 nm). Representative AFM height images (2.5 μm × 2.5 μm) of nanoparticles that were formed after O_2 and N_2 plasma treatments are shown in Figure 1a,b, respectively. As measured from the AFM height images, the average height of the Ga_2O_3 nanoparticles obtained from O_2 plasma and the corresponding value for GaN nanoparticles obtained from N_2 plasma were 4.2 ± 0.4 nm and 4.4 ± 0.4 nm, respectively. The average distance between the nanoparticles was around 45−50 nm. Moreover, there was no noticeable difference in the nanoparticles that formed on different substrates (Si, sapphire, fused silica glass). The two-dimensional fast Fourier transform (FFT) image, shown as an inset in Figure 1b, showed arrangement of nanoparticles along a hexagonal lattice and the appearance of the second order intensity peaks in the FFT spectrum indicated ordered arrangement of the nanoparticles.

Finally, arrays of oxide nanoparticles were treated with ammonia in a CVD reactor at temperatures in the range 600−850 °C at atmospheric pressure to grow crystalline GaN

nanocrystals using two slightly different methods. In the first method, gallium oxide nanoparticles were directly treated with ammonia gas at reaction temperatures to form GaN nanocrystals. In the second method, gallium oxide nanoparticles were first reduced using H_2 gas to form Ga (liquid), which was then treated with ammonia to form GaN. The N_2 plasma treatment resulted in a mixture of amorphous and crystalline GaN nanoparticles, requiring an annealing treatment at higher temperatures to improve their crystallinity.

Gallium oxide nanoparticles obtained by O_2 plasma treatment were treated with ammonia using two different methods in a thermal CVD. Both methods were performed at ambient pressure with temperature ranges of 600−800 °C in a 2.5 cm diameter quartz tube with a 37.5 cm heating zone. In the first method (Method 1), substrates with Ga_2O_3 nanoparticles (obtained from GaAc salt-loaded polymer micelles) were heated from room temperature to the growth temperature in a flow of argon gas (600 sccm). Subsequently, nitride growth was initiated by adding ammonia (60−100 sccm) to the argon gas flow and continued for 15 min. The growth was terminated by switching off the ammonia flow, and the samples were cooled in an argon gas flow. In the second method (Method 2), all the steps were similar except the first step, where the nanoparticle-coated substrates were heated to final growth temperatures in a gas mixture of argon (600 sccm) and hydrogen (100 sccm). Syntheses of bulk GaN from bulk samples of Ga_2O_3 as well from as from liquid Ga using ammonia gas have been previously reported.[21−22] The two different synthesis methods involve different sets of reactions for the formation of GaN and are believed to occur as per the following reactions:

$$\text{Method 1: } Ga_2O_3 + 2NH_3 \rightarrow 2GaN + 3H_2O \quad (1)$$

$$\text{Method 2: } Ga_2O_3 + 3H_2 \rightarrow 2Ga + 3H_2O \quad (2\text{-i})$$

$$2Ga + 2NH_3 \rightarrow 2GaN + 3H_2 \quad (2\text{-ii})$$

In another experiment (Method 3), N_2 plasma was first used to remove the polymeric shell, and the samples were then subsequently annealed in a flow of ammonia gas at temperatures in the range of 650−700 °C to form crystalline GaN nanoparticles.

Transmission electron microscopy (TEM) data was collected using a JEOL 2010, operating at 200 kV. Plan view TEM samples of GaN nanocrystals on Si substrates were prepared as previously reported.[19] A representative TEM image of GaN nanocrystals after ammonia treatment of nanoparticles obtained from oxygen plasma treatment, using Method 2 at 650 °C, is shown in Figure 1c. A TEM image of GaN nanocrystals after ammonia treatment of nanoparticles obtained from nitrogen plasma treatment, using Method 3, is shown in Figure 1d. Additional TEM images of GaN nanocrystals on a Si substrate are provided in the Supporting Information. The arrangement of nanocrystals was unaffected even after ammonia treatments suggesting that the nanoparticles are stable at these high temperatures. Representative lattice-resolved images and of the GaN nanoparticles corresponding to samples described above are

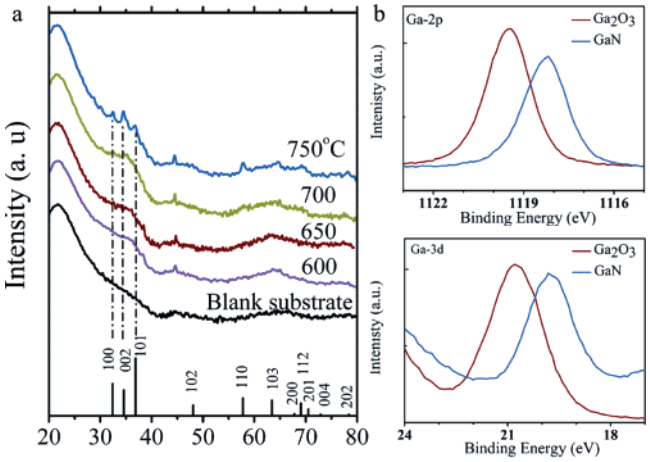

Figure 2. (a) XRD patterns from multilayered GaN nanoparticles on quartz substrates synthesized by ammonia CVD of Ga_2O_3 nanoparticles at different temperatures. The diffraction peaks corresponding to bulk GaN (JCPDS card number: 50−0792) are also provided for reference. (b) High-energy resolution XPS spectra of Ga-$2p_{3/2}$ (above) and Ga-$3d_{5/2}$ (below) before (Ga_2O_3) and after (GaN) ammonia treatment of Ga_2O_3 nanoparticles.

shown in Figure 1e,f, respectively, which revealed their crystallinity. The FFTs of crystalline nanoparticles are provided as insets. Using nitrogen plasma as compared to oxygen plasma to remove the polymeric shell would be advantageous for the following reasons: first, absence of oxygen in the precursor material would result in pure GaN nanoparticles, and second the crystallinity of GaN nanoparticles is likely to be better than in the latter case due to the absence of a significant change in volume associated with the different types of chemical bonds (Ga−O versus Ga−N). Thus, the TEM data not only revealed the crystalline nature of nitride nanoparticles but also indicated that the periodicity and the arrangement of nanocrystals were unaffected at higher growth temperatures. Synthesis of amorphous GaN by thermal decomposition of cyclotrigallazane directly within the polymer solutions had been previously reported.[12] Decomposition temperatures of cyclotrigallazane were limited to low temperature (180 °C) as the entire synthesis was performed in the polymer matrices, which only resulted in the formation of amorphous GaN. Here, the removal of polymeric template after the initial processing steps enabled us to employ higher reaction temperatures with ammonia resulting in crystalline GaN nanoparticles.

The crystal structure of GaN nanocrystals synthesized using methods described above was ascertained using X-ray diffraction (XRD) analysis. XRD spectra were collected on a Rigaku X-ray powder diffractrometer operating at 50 kV and with a current of 200 mA with a Cu-Kα radiation. XRD samples were prepared by vacuum-drying a droplet of the micellar solution on fused silica glass substrates for a few hours prior to oxygen plasma treatment. Subsequently, ammonia treatment was employed to synthesize GaN nanoparticles at the same conditions as previously described. Figure 2a shows the XRD diffraction patterns measured in the 2θ range of 20−80° from multilayered GaN samples synthesized in the temperature range of 600−800 °C. The

fractional area occupied by GaN nanoparticles on the substrates was low (fractional area was $\sim 10^{-3}$% for a particle density of $\sim 10^{11}/cm^2$ on the substrate and with an average diameter of 5 nm), and hence a high background signal from the substrate was observed in the diffraction patterns. The diffraction peak at 44.5° in all the samples might have risen from the impurities in the precursor. The diffraction pattern from the blank substrate is also displayed in the same figure for comparison. XRD patterns collected from GaN samples synthesized at temperatures in the range of 600−750 °C exhibited evolution of spectra from broad to fine peaks with increasing temperature, suggesting improvement in the crystallinity. The XRD peaks of the sample synthesized at 750 °C are in agreement with the diffraction peaks from wurtzite bulk GaN, indicating a wurtzite crystal structure for a majority of these nanoparticles.

The chemical states of the nanoparticles prior to and after the nitride growth of gallium oxide nanoparticles were determined using X-ray photoelectron spectroscopic (XPS) analysis. XPS data were collected on a Kratos Axis 165, using a monochromatic Al Kα with photon energy of 1486.6 eV. Carbon-1s peak was used as an internal reference for the energy calibration of the high-resolution spectra. Figure 2b,c shows the high-resolution spectra of Ga-2$p_{3/2}$ and Ga-3$d_{5/2}$ peaks, respectively, from the sample before and after nitride growth at 650 °C using Method 1. The presence of Ga-2p and Ga-3d peaks at 1119.5 and 20.8 eV, respectively, for the sample after oxygen plasma treatment indicated that Ga was present in the form of Ga_2O_3.[23−24] Following ammonia treatment, the corresponding Ga peaks are present at 1118.2 and 19.6 eV, indicating the formation of nitride.[25−26] The lowering of binding energy for the Ga-2p and Ga-3d peaks, in the case of Ga−N type bonding as compared to the Ga−O bonding, were consistent with the lower electronegativity of nitrogen compared to that of oxygen. Ga-2p and Ga-3d peak shifts from Ga−O to Ga−N type bonding were 1.3 and 1.2 eV, respectively, and these shifts in the binding energy are also in close agreement with a previous report.[27]

Interestingly, ammonia treatment of Ga_2O_3 nanoparticles at temperatures above 750 °C resulted in the formation of nanowires with a decrease in the density of nanoparticles (see Supporting Information), suggesting that Ga_2O_3 nanoparticles acted as self-catalysts for the growth of GaN nanowires. This hypothesis was further confirmed by growing the nitride nanowires from Ga_2O_3 nanoparticles in the presence of an additional source of Ga (GaAc salt on a Si substrate, which was placed upstream at a distance of 20 cm away from the Ga_2O_3 nanoparticles containing substrate). The additional Ga source resulted in observation of a higher density of nanowires as shown in a scanning electron microscopy (SEM) image (Supporting Information, Figure 2). These results indicate that treatment of Ga_2O_3 nanoparticles with ammonia can be tailored to achieve either GaN nanocrystals in the temperature range 600−750 °C or GaN nanowires in the presence of an additional source of Ga at temperatures exceeding 750 °C (see Supporting Information, Figure 3 for XRD patterns of GaN nanowires).

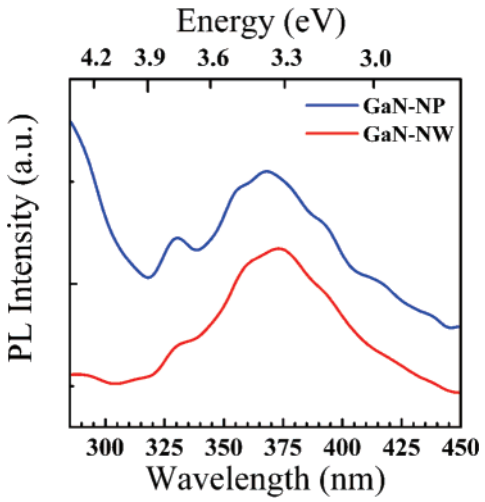

Figure 3. Room-temperature PL spectra of GaN nanocrytsals on Si substrate synthesized using Method 2 at 650 °C (above spectrum) GaN nanowires on Si substrate synthesized at 750 °C using Ga_2O_3 nanoparticles as self-catalysts (below).

Photoluminescence (PL) spectral data of GaN nanoparticles on Si substrates were collected at room temperature, excited by a monochromatic source with an excitation energy of 4.77 eV (260 nm), and obtained from a Xenon lamp using Horiba Jobin Yvon spectrophotometer (Nanolog). The PL spectrum (Figure 3) from GaN nanoparticles synthesized using Method 2 at 750 °C showed a broad peak centered at 370 nm (3.35 eV) and a small, narrow peak at 330 nm (3.75 eV). We believe the broad spectral peak arose due to the absence of surface passivation of the nanocrystals. The small peak at 330 nm (3.75 eV) with a full width at half-maximum about 330 meV demonstrated a blue-shift in the emission photon energy of nanoparticles compared to the band gap of bulk GaN (Wurtzite: 3.4 eV), indicating that the emission peak resulted from the quantum confined states in GaN nanoparticles. Similarly, a blue-shifted emission peak at 329 nm (3.769 eV) was observed in PL spectrum of GaN nanowires (Figure 3), again a result of the quantum confinement effects.

On the other hand, synthesis of InN nanoparticles is an interesting prospect for a number of reasons. For example, even as of today the actual band gap of bulk InN is still a subject of debate; recent reports on the band gap of InN (0.7−1.1 eV)[28] are in sharp contrast to earlier cited reports (1.8−2.0 eV).[29] In addition, it has rather been difficult to synthesize pure InN for several reasons: (a) a need for higher equilibrium vapor pressure of nitrogen as compared to that of other nitrides; (b) a need for lattice-matched substrates; and (c) lower decomposition temperature of InN (∼500−700 °C).[30] InN nanocrystals on various substrates were synthesized using a similar method described above for GaN nanocrystals. Indium acetyl acetonoate salt was loaded in the PS-P4VP polymer micelles, and the micellar solution was spin-coated on substrates and subsequently, nitrogen plasma (350−400 mtorr, 5 min) was used to remove the polymer shell that also resulted in the formation of InN nanoparticles. Finally, the nitride nanoparticles containing substrates were annealed in ammonia gas (NH_3/Ar: 60/600 sccm) at tem-

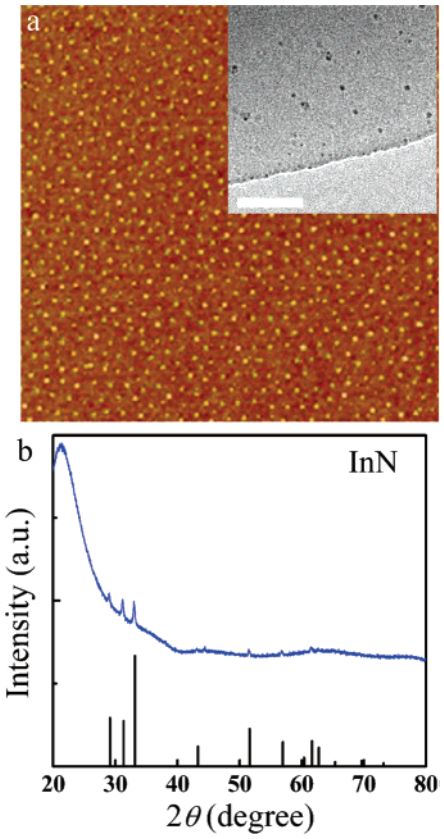

Figure 4. (a) An AFM image (1.25 μm × 1.25 μm) of InN nanocrystals on Si substrate (inset is a TEM image of InN nanocrystals that were annealed in NH_3 at 550 °C, scale bar 50 nm). (b) XRD pattern from a multilayer of InN nanocrystals on fused silica substrate. The diffraction peaks corresponding to bulk wurtzite InN (JCPDS card number: 50−1239) are also provided for reference.

peratures in the range of 550−600 °C to further improve their crystallinity. Figure 4a shows AFM height image (1.25 μm × 1.25 μm) of InN nanoparticles after N_2 plasma treatment, and a corresponding TEM image of InN nanocrystals after annealing in ammonia is shown as an inset in the same figure. XRD diffraction pattern collected from a multilayered sample on fused silica substrate that was annealed at 550 °C indicated a wurtzite crystal structure for the InN nanoparticles. Thus, TEM data in conjunction with the XRD results confirmed the synthesis of InN nanocrystals. These results demonstrated that the PS-P4VP block copolymer method offers a promising route for the synthesis of III-nitrides. Examinations on the PL emission spectra from InN nanocrystals on silicon and sapphire substrates are currently under investigation in our laboratory.

In summary, synthesis of ordered arrays of monodisperse GaN and InN nanocrystals using PS-P4VP block copolymer templates is demonstrated. Structural and chemical characterizations confirmed wurtzite crystal structure for both GaN and InN nanoparticles and the PL emission spectra of GaN nanostructures indicated a blue-shift in the photon emission energy compared to bulk wurtzite GaN, a result of quantum confined states in the nanostructures. A unique advantage of this method features synthesizing monodisperse arrays of nanoparticles with simultaneous control over their size and the periodicity. This method not only offers promise for the controlled synthesis of ternary III-N nanocrystals but may also enable doping of III-nitride nanostructures.

Acknowledgment. The authors thank Professor Jing Kong for sharing her CVD facility and Dr. Christine Flynn for useful comments. Center of Materials Science and Engineering (CMSE) experimental facilities were extensively used in this work. This work was supported by DARPA joint ATO DSP grant, the National Institute of Health, and National Cancer Institute, Center of Cancer Nanotechnology Excellence (CCNE).

Supporting Information Available: Additional TEM images of GaN nanocrystals on Si substrate, SEM data of GaN nanowires, and infrared spectra of metal precusor-P4VP solutions are provided. XRD data of GaN nanowires is also provided.

References

(1) Ponce, F. A.; Bour, D. P. *Nature* **1997**, *386*, 351−359.
(2) Nakamura, S. *Annu. Rev. Mater. Sci.* **1998**, *28*, 125−152.
(3) (a) Johnson, J. C.; Choi, H. C.; Knutsen, K. P.; Schaller, R. D.; Yang, P.; Saykally, R. J. *Nat. Mat.* **2002**, *1*, 106−110. (b) Hwang, Y.; Duan, X.; Cui, Y.; Lauhon, L. J.; Kim, K. H.; Lieber, C. L. *Science* **2001**, *294*, 1313−1317.
(4) Micic, O. I.; Ahrenkiel, S. P.; Bertram, D.; Nojik, A. J. *Appl. Phys. Lett.* **1999**, *75*, 478−480.
(5) Preschilla, N. A.; Major, S.; Kumar, N.; Samajdar, I.; Srinivasa, R. S. *Appl. Phys. Lett.* **2000**, *77*, 1861−1863.
(6) Xie, Y.; Qian, Y.; Wang, W.; Zhang, S.; Zhang, Y. *Science* **1996**, *272*, 1926−1927.
(7) Sardar, K.; Rao, C. N. R. *Adv. Mater.* **2004**, *16*, 425−429. (b) Sardar, K.; Dan, M.; Schwenzer, B.; Rao, C. N. R. *J. Mater. Chem.* **2005**, *15*, 2175−2177.
(8) Hwang, J.; Campbell, J. P.; Kozubowski, J.; Hanson, S. A.; Evans, J. F.; Gladfelter, W. L. *Chem. Mater.* **1995**, *7*, 517−525.
(9) Frank, A. C.; Stowasser, F.; Sussek, H.; Pritzkow, H.; Miskys, C. R.; Ambacher, O.; Giersig, M.; Fischer, R. A. *J. Am. Chem. Soc.* **1998**, *120*, 3512−3513.
(10) (a) Janik, J. F.; Wells, R. L. *Inorg. Chem.* **1997**, *36*, 4135−4137. (b) Jegier, J. A; McKerman, S.; Purdy, A. P.; Gladfelter, W. L. *Chem. Mater.* **2000**, *12*, 1003−1010.
(11) Leppert, V. J.; Murali, A. K.; Risbud, S. H.; Stender, M.; Power, P. P.; Nelson, C.; Banerjee, P.; Mayes, A. M. *Philos. Mag. B* **2002**, *82*, 1047−1054.
(12) Azuma, Y.; Shimada, M.; Okuyama, K. *Chem. Vap. Deposition* **2004**, *10*, 11−13.
(13) Daudin, B.; Widmann, F.; Feuillet, G.; Adelmann, C.; Samson, Y.; Arlery, M.; Rouviere, J. L. *Mater. Sci. Eng., B* **1997**, *50*, 8−11.
(14) Park, M.; Harrison, C.; Chaikin, P. M.; Register, R. A.; Adamson, D. H. *Science* **1997**, *276*, 1401−1404.
(15) (a) Thurn-Albrecht, T.; Schotter, J.; Kastle, G. A.; Emley, N.; Shibauchi, T.; Krusin-Elbaum, L.; Guarini, K.; Black, C. T.; Tuominen, M. T.; Russel, T. P. *Nature* **2000**, *15*, 2126−2129. (b) Guarini, K. W.; Black, C. T.; Zhang, Y.; Kim, H.; Sikorski, E. M.; Babich, I. V. *J. Vac. Sci. Technol., B* **2002**, *20*, 2788−2792.
(16) Antonietti, M.; Wenz, E.; Bronstein, L.; Seregina, M. *Adv. Mater.* **1995**, *7*, 1000−1005.
(17) Spatz, J. P.; Mossmer, S.; Hartmann, C.; Moller, M. *Langmuir* **2000**, *16*, 407−415.
(18) Glass, R.; Moller, M.; Spatz, J. P. *Nanotechnology* **2003**, *14*, 1153−1160.
(19) Bhaviripudi, S.; Reina, A.; Qi, J.; Kong, J.; Belcher, A. M. *Nanotechnology* **2007**, *20*, 5080−5086.
(20) Belfiore, L. A.; Pires, A. T. N.; Wang, Y.; Graham, H.; Ueda, E. *Macromolecules* **1992**, *25*, 1411−1419.
(21) Johnson, W. C.; Parsons, J. B.; Crew, M. C. *J. Phys. Chem.* **1932**, *36*, 2651−2654.

(22) Schoonmaker, R. C.; Burton, C. E. *Inorg. Synth.* **1962**, *7*, 16−18.
(23) Moulder, J. F.; Stickle, W. F.; Sobol, P. E.; Bomben, K. D. *Handbook of X-ray Photoelectron Spectroscopy*; Physical Electronics: Eden Prairie, MN, 1995.
(24) Carli, R.; Bianchi, C. L. *App. Surf. Sci.* **1994**, *74*, 99−102.
(25) Hedman, J.; Martensson, N. *Phys. Scr.* **1980**, *22*, 176−178.
(26) Carin, R.; Deville, J. P.; Werckman, J. *Surf. Interface Anal.* **1990**, *16*, 65−69.
(27) Wolter, S. D.; Luther, B. P.; Waltemyer, D. L.; Onneby, C.; Molnar, R. J. *Appl. Phys. Lett.* **1997**, *70*, 2156−2158.
(28) Xu, K.; Yoshikawa, A. *Appl. Phys. Lett.* **2003**, *83*, 251−253.
(29) (a) Tansley, T. L.; Foley, C. P. *J. Appl. Phys.* **1986**, *59*, 3241−3244. (b) Wu, J.; Walukeiewicz, W.; Yu, K. M.; Ager, J. W., III; Haller, E. E.; Lu, H.; Schaff, W. J.; Saito, Y.; Nanishi, Y. *Appl. Phys. Lett.* **2002**, *80*, 3967−3969.
(30) Schwenger, B.; Loeffler, L.; Seshadri, R.; Keller, S.; Lange, F. F.; Denbaars, S. P.; Mishra, U. K. *J. Mater. Chem.* **2004**, *14*, 637−641.

NL072129D